Published in final edited form as:
FEBS J. 2012 August ; 279(16): 2892–2904. doi:10.1111/j.1742-4658.2012.08669.x.

A role for γS-crystallin in the organization of actin and fiber cell maturation in the mouse lens

Jianguo Fan[1,*], **Lijin Dong**[1,*], **Sanghamitra Mishra**[1], **Yingwei Chen**[1], **Paul FitzGerald**[2], and **Graeme Wistow**[1]

[1]Section on Molecular Structure and Functional Genomics, National Eye Institute, National Institutes of Health, Bethesda, MD, USA

[2]Department of Cell Biology and Human Anatomy, School of Medicine, University of California, Davis, CA, USA

Abstract

γS-crystallin (γS) is a highly conserved component of the eye lens. To gain insights into the functional role(s) of this protein, the mouse gene (*Crygs*) was deleted. Although mutations in γS can cause severe cataracts, loss of function of γS in knockout (KO) mice produced no obvious lens opacity, but was associated with focusing defects. Electron microscopy showed no major differences in lens cell organization, suggesting that the optical defects are primarily cytoplasmic in origin. KO lenses were also grossly normal by light microscopy but showed evidence of incomplete clearance of cellular organelles in maturing fiber cells. Phalloidin labeling showed an unusual distribution of F-actin in a band of mature fiber cells in KO lenses, suggesting a defect in the organization or processing of the actin cytoskeleton. Indeed, in wild-type lenses, γS and F-actin colocalize along the fiber cell plasma membrane. Relative levels of F-actin and G-actin in wild-type and KO lenses were estimated from fluorescent staining profiles and from isolation of actin fractions from whole lenses. Both methods showed a twofold reduction in the F-actin/G-actin ratio in KO lenses, whereas no difference in tubulin organization was detected. *In vitro* experiments showed that recombinant mouse γS can directly stabilize F-actin. This suggests that γS may have a functional role related to actin, perhaps in ‘shepherding’ filaments to maintain the optical properties of the lens cytoplasm and normal fiber cell maturation.

Keywords

actin cytoskeleton; crystallins; knock-out mouse; organelles

Introduction

The vertebrate lens is a highly organized system of regularly packed cells with high concentrations of proteins, forming a transparent tissue with a gradient of refractive index that eliminates diffraction and aberration errors and produces the fine focus required for vision [1–3]. Transparency along the optical axis of the lens is enhanced by elimination of cellular organelles in mature fiber cells [4]. The refractive index gradient is produced by developmentally regulated layering and packing of elongated fiber cells and stage-specific expression of the proteins in those cells [2,4–7]. At the molecular level, the bulk of the

Correspondence: G. Wistow, Section on Molecular Structure and Functional Genomics, National Eye Institute, Bg 6, Rm 106, National Institutes of Health, Bethesda, MD 20892-0608, USA, Fax: +1 301 496 0078, Tel: +1 301 402 3452, graeme@helix.nih.gov.
*These authors contributed equally to this work

refractive index of the lens is attributable to the highly abundant, soluble crystallins. During the evolution of the vertebrate eye, crystallins arose by recruitment of pre-existing proteins, probably with ancient roles in other parts of the eye [8–10]. Indeed, the optical properties of the lens in different vertebrate lineages have frequently been adjusted by the independent recruitment of proteins such as enzymes as novel crystallins [11,12].

The α-crystallins, which are present in all vertebrates, are derived from small heat shock proteins and have roles as molecular chaperones [13–15]. The β-crystallins and γ-crystallins are also represented throughout vertebrate evolution, and must have formed part of the earliest vertebrate lenses [16,17]. They are related in sequence and structure, and form part of the wider βγ-crystallin superfamily, which includes proteins ranging from a bacterial spore coat protein [18] to a mammalian protein implicated in the control of metastasis in melanoma [19]. β-Crystallins have orthologs in species from fish to mammals; however, γ-crystallins are much more variable, and seem to have been particularly subject to adaptation, duplication and gene loss in different vertebrate lineages [16].

One member of the family, γS-crystallin (γS), is well conserved in evolution, and has orthologs and paralogs in fish, mammals, reptiles, and birds [16], making it a candidate representative for an ancient, functional role of γ-crystallins in the eye. Expression of γS has been observed in non-lens eye tissues [20]. It appears to be subject to light–dark cycle regulation in the retina [21]; it is induced in an aging model of retinal pigment epithelium [22]; and it is abundant in drusen [23,24], suggesting possible involvement in age-related macular degeneration.

Mutations in γS cause cataracts in both mice and humans [25–27]. In the murine *Opj* cataract, a temperature-sensitive mutation leads to unfolding of γS, and produces opacity, with severe disruption of lens cell organization [26]. *Opj* involves both loss of function and the toxic effects of an abundant, misfolded protein that is capable of forming amyloid-like fibrils both *in vivo* and *in vitro* [28,29]. To separate loss and gain of function effects and to provide insights into the functional roles of γS, the mouse *Crygs* gene was deleted by homologous recombination.

Results

Creation of *Crygs* null allele

The promoter and exon 1 of *Crygs* in an SV129 BAC clone containing murine *Crygs* was replaced by a *Neo* cassette (Fig. 1A). The deletion construct was electroporated into SV129 ES cells and selected for G418 resistance. A homologous recombinant clone line was identified by Southern blotting (Fig. 1B), and was injected into C57Bl/6 blastocysts to produce chimeric embryos. Germ line transmission of the deletion allele was established through subsequent breeding with C57Bl/6. Heterozygous (+/−) mice were crossed with C57Bl/6 for multiple generations (currently 10) to achieve a uniform genetic background. Mice were genotyped for the lens cytoskeleton protein CP49/BFSP2, because SV129 mice contain a mutation in this gene [30,31].

Validation of the knockout (KO)

γS mRNA in wild-type (WT) (+/+), heterozygous (+/−), KO (−/−) and *Opj* (γS mutant) lenses was examined by RT-PCR (Fig. 2A). No expression was observed in the KO lens. Lenses from the same genotypes, separated into water-soluble, mild detergent (Triton)-soluble and SDS-soluble fractions, were examined by western blot. γS protein was absent from the KO lens. The protein was detected in all three fractions of +/+ and +/− lenses, showing that some γS is associated with insoluble membrane/cytoskeletal fractions (Fig. 2B). For the *Opj* mutant lens, most of the γS protein was found in the highly insoluble SDS-

extracted fraction, but no mutant protein was present in the cytoskeleton-associated Triton fraction. The migration of γS protein in the Triton and SDS fractions appeared to be slightly retarded, although the control western blot for macrophage migration inhibition factor [32] from the same fractions showed identical mobility in all cases. The reason for this shift is unknown.

Protein content of the KO lens

Total soluble protein content was measured for WT, KO and *Opj* lenses (Fig. 2C). Whereas the amount of soluble protein in the *Opj* lens was severely reduced, both WT and KO lenses had similar levels. WT and KO lens proteins were separated by 2D gel electrophoresis. Figure 3A shows that silver stain profiles for both were remarkably similar, with changes only in the 10–20-kDa range. The major missing spot in the KO lens corresponds to the expected position for γS [33]. Several smaller spots with different charge characteristics were also missing in the KO lens. γS protein undergoes post-translational changes with aging in the lens [34]. Figure 3B,C shows the Coomassie stain and γS western blot for duplicate blots. No γS immunoreactivity was present in the KO lens, but multiple γS-derived spots were detected in the WT lens, corresponding to spots missing in the silver stain pattern. As the antiserum against γS was raised against a peptide in the C-terminal domain [20], additional N-terminal domain fragments could also exist.

Optical properties of the KO lens

In contrast to the severe cataract resulting from mutation of γS in the *Opj* lens [26], the KO lens had no major opacity. Figure 4 shows photographs of littermate WT and KO lenses under identical conditions. Up to 1 year of age, the WT lens is clear and the KO shows, at most, a slight haziness with no cataract. However, a greater difference is seen when lenses are used to visualize an object under the dissecting microscope. Up to 3 months, there is no difference in image formation between WT and KO lenses. With age, even in the WT lens, the sharpness of focus decreases, but this is much more noticeable in the KO lens: by 8 months, image formation is blurred and distorted.

Lens structure and histology

Scanning electron microscopy (SEM) and transmission electron microscopy (TEM) showed no differences in cell shape or organization in the KO lens (Fig. 5). Light microscopy also showed that WT and KO lenses were similar in size and general appearance at all ages examined. However, in adult lenses (4 months and older), 4′,6-diamidino-2-phenylindole (DAPI) staining of cell nuclei showed that, whereas the onset of nuclear breakdown that occurs in maturing cortical fiber cells was similar in WT and KO lenses, scattered fragments of nuclear debris persisted in deeper layers of mature fiber cells in the KO lens, becoming particularly noticeable by 6 months (Figs 6A and 7). Similarly, labeling for markers for mitochondria and endoplasmic reticulum, which are also cleared from maturing fiber cells, revealed persistence of these markers in mature cell layers (Fig. 6B). The distributions of the lens-specific intermediate filament proteins BFSP1 (filensin) and BFSP2 (CP49) [35,36] showed no differences between WT and KO lenses (Fig. 6C).

Actin distribution

Phalloidin staining for F-actin showed a marked difference between WT and KO lenses (Fig. 7). Whereas the WT lens had fairly uniform staining throughout the cortical fiber cells, the KO lens showed a distinct band of cell layers in the deep cortical region with uneven staining of F-actin. This band of unusual phalloidin staining was seen consistently in KO lenses ranging from 6 months to > 1 year of age, but was not noticeable in younger lenses. Examination of the 2D gels of lens proteins in the actin size range (43 kDa) showed no

major differences between WT and KO lenses (Fig. 3), suggesting that this difference results from post-translational events. The basis for the uneven phalloidin staining is not known. However, it is unlikely to be associated with the formation of large aggregates, as these would be expected to cause light scattering and opacity. Furthermore, TEM of lens fibers showed no evidence of large aggregates (Fig. 5). Nevertheless, it appeared that the organization of actin in the fiber cells of the γS KO lens might be abnormal.

Alteration in the F-actin/G-actin ratio in the γS KO lens

Multiple littermate WT and KO lens sections from 6- to 8-month-old mice were dual-labeled with phalloidin (for polymerized F-actin) and with fluorescently labeled DNaseI (for monomeric G-actin), and the relative fluorescence intensities were scanned from the epithelium into the cortical lens fibers (Fig. 8). The ratio of F-actin/G-actin staining intensity, averaged over 300 nm into the lens cortex, was two-fold higher in the WT lens than in the KO lens.

F-actin and G-actin fractions from multiple whole WT and KO lenses were quantitated by western blotting (Fig. 9A,B). This approach also showed a twofold decrease in the F-actin/G-actin ratio in the KO lens. Western blots for total actin in whole lens homogenized in RIPA buffer showed no significant difference between littermate WT and KO pairs (Fig. 9C). Also, no difference was detected in the polymerized/unpolymerized ratio for tubulin in WT and KO lenses (Fig. 9D,E).

γS was localized in thick sections of the WT mouse lens that were partially ‘ghosted’ to reduce the strong signal from cytoplasmic protein. As shown in Fig. 10A, both antibody against γS and antibody against phalloidin showed colocalization along the plasma membrane. Furthermore, γS could be detected in the pellet fraction of whole WT lenses, but this was almost abolished by the addition of cytochalasin D, which depolymerizes F-actin (Fig. 10B).

Effect of γS-crystallin on the stability of F-actin

Recombinant mouse γS was used in *in vitro* polymerization and depolymerization assays with fluorescently labeled actin [37,38]. As shown in Fig. 11, addition of γS had no significant effect on the rapid polymerization of actin. However, in depolymerization assays, γS showed a significant, concentration-dependent stabilization of preformed F-actin, whereas BSA (at 100 μg) showed little stabilization, similar to buffer alone.

Discussion

γ-Crystallins constitute a family of highly specialized proteins that have evolved as major components of the refractive structure of the vertebrate eye lens. The mouse lens expresses eight different γ-crystallins: γA-crystallin (γA), γB-crystallin (γB), γC-crystallin (γC), γD-crystallin (γD), γE-crystallin (γE), γF-crystallin (γF), γS, and γN-crystallin (γN) [16,39]. The genes for γA–γF are clustered on mouse chromosome 1, and are expressed at their highest levels in the fiber cells of the embryonic lens [11,40]. These cells form the lens nucleus, the densest, highest refractive index part of the mature lens [2,40]. The recently discovered γN is expressed at relatively low levels, but is also found predominantly in the lens nucleus [16]. Interestingly, γE, γF and γN are all encoded by pseudogenes in humans, whereas γA and γB are expressed at only low levels [16,41,42]. γD–γF are also apparently absent from the guinea pig, suggesting that several of these proteins are functionally dispensable [43]. Indeed, γA–γF have no orthologs in nonmammalian species; fish have multiple γM proteins that are only distantly related to mammalian γ-crystallins [16].

In contrast, γS is well conserved throughout vertebrate evolution [16], and, unlike the other γ-crystallins, is expressed at high levels in cortical fiber cells and even in lens epithelium [44]. It is not lens-specific; being expressed at lower levels in cornea and retina, but, overall, it is shows a high preference for the eye in expression [20,21,45]. Along with some α-crystallins and β-crystallins, γS has been detected in drusen, plaque-like deposits in Bruch's membrane, basal to the retinal pigment epithelium, which are associated with age-related macular degeneration [23]. It is also induced in an animal model of retinal pigment epithelium damage [22]. These observations hint that γS may retain an ancestral functional role that may have first been important in the retina and other parts of the eye, perhaps as a stress protein, even before the later evolution of the vertebrate lens. This original function may have been selectively useful in the lens, and may underlie the recruitment of γ-crystallins to the ancestral vertebrate lens [17].

The γS KO lens has a slight haziness but no major opacity. This contrasts with the very severe *Opj* cataract, in which misfolding/unfolding of mutant γS leads to disruption of the cell architecture and fibril formation [26,28,29,46]. The mild γS KO phenotype also contrasts with that produced by deletion of a major β-crystallin, βB2, in which age-related cataract is reported [47]. However, whereas deletion of γS causes no acute loss of transparency, the optical properties of the maturing KO lens are defective and image formation is poor as compared with the matched WT lens (up to 1 year of age, the KO mice show no obvious differences in nonlens eye tissues, where γS is expressed at much lower levels than in the lens).

In normal vertebrate lens development, maturing fiber cells undergo a tightly regulated process of loss of nuclei, mitochondria, and other organelles [4]. It is believed that this may have evolved to reduce light scattering along the visual axis of the lens. In maturing fiber cells, nuclei condense and undergo chromatin degradation in a process reminiscent of apoptosis [48,49]. In the young lens, the nuclear debris is substantially cleared within a few layers of fiber cells (although this clearance seems to become less efficient with age). However, in several cataracts and in the DNaseIIβ null mouse [4,50], the program of nuclear and other organelle breakdown is deficient to varying degrees. This is also seen in the γS KO lens, with persistence of DAPI-positive bodies, which are presumably fragments of condensed chromatin- containing structures, deep into cortical layers. Labeling of markers for mitochondria and the endoplasmic reticulum also suggests that clearance of these organelles may be defective in the KO lens. This raises the possibility that γS participates in normal functioning of the machinery of cell maturation, perhaps through interactions with components of intracellular trafficking, such as intermediate filaments and microtubules.

Indeed, the KO lens exhibits a well-defined zone of mature fiber cells in the deep cortical region of the lens, in which phalloidin staining shows an uneven distribution of F-actin. The vertebrate lens contains several discrete developmental zones marked by changes in fiber cell structure, organelle and cytoskeleton organization, and specific patterns of gene expression [1,4,6,7,51]. The KO lens may contain a region in which reorganization of the actin cytoskeleton is defective.

Indeed, quantitation of the ratio of polymeric F-actin to monomeric G-actin in the lens by two methods showed consistent differences between WT and KO lenses, with an overall two-fold decrease in the F-actin/G-actin ratio in the KO lens, but no difference in overall levels of expressed actin. This suggests that γS may be required for normal regulation of F-actin levels in the mouse lens. In contrast, no difference was detected in the organization of tubulin in the WT and KO lenses.

Actin filaments constitute a key part of the architecture of the cell, and serve to anchor and localize other components with various functions, including cell–cell junctional complexes, and also form part of the contractile systems for cell motility [52]. Light and electron microscopy showed no evidence of major defects in cell shape or packing in the KO lens, suggesting that any difference in actin organization associated with the absence of γS is not sufficient to affect the machinery of fiber cell elongation or the formation of cellular junctions. The effect of the absence of γS appears to be concentrated in the organization of the fiber cell cytoplasm.

Recombinant mouse γS was tested for its ability to alter rates of polymerization or depolymerization of pyrene-labeled actin, as detected by increased fluorescence in the polymerized state. No effect was seen on the rapid polymerization of actin, but γS significantly slowed the depolymerization of F-actin in a concentration-dependent manner. This occurred at approximately stoichiometric levels, which are certainly achievable in the normal lens, where γS abundance is at least equivalent to that of actin, as is apparent from Fig. 3 and from proteome analysis [53].

Although γS is able to stabilize F-actin, this may not involve direct tight binding, as experiments including yeast two-hybrid screening have failed to identify any strong binary interaction of γS with another protein (unpublished data). However, the WT lens does contain a fraction of γS that, under nondenaturing conditions, is associated with material that pellets under centrifugation, and this fraction is greatly reduced in the presence of cytochalasin D. Together with evidence for colocalization of γS and F-actin in fiber cells, this suggests that some γS is associated with F-actin in lens.

Is a role for γS in actin organization or stabilization plausible from a wider evolutionary and superfamily perspective? β-Crystallins and γ-crystallins are both related to a number of nonlens proteins in prokaryotes and eukaryotes [8,19,54]. Although the functions of these proteins are not well understood, some of them do have plausible connections with the cytoskeleton and/or control of cell morphology. For example, expression of AIM1 (absent in melanoma 1, which contains six γB domains) is associated with a change in morphology and invasiveness in melanoma cells [19], whereas EDSP (Ep36) is closely associated with the plasma membrane in developing newt larvae [55,56]. Lens fiber cells undergo a huge increase in size as they differentiate from epithelial cells, and this involves a massive elaboration of the cytoskeleton. During evolution, there could have been selective advantages to the recruitment of proteins to the lens that would be beneficial in these processes. Indeed, there is evidence the α-crystallins, members of the small heat shock protein superfamily, also have functional associations with the lens cytoskeleton [57–59]. The KO model suggests that γS, too, may have a role in maintaining the optimal organization of F-actin in the lens cell cytoplasm. The same sort of ‘shepherding’ functionality could also be involved in maintaining the short-range order of the multimeric complexes of α-crystallins and β-crystallins in the lens [40,60].

Experimental procedures

Construction of the *Crygs* null allele

The 5′-flank and exon 1 of the mouse *Crygs* gene in a BAC clone (#20750; Genome Systems, St Louis, MO, USA) were replaced by a *Neo* selectable marker cassette [61]. The construct was electroporated into ES cells (SV129), and G418-resistant clones were screened for homologous recombination by Southern blotting with a 5′-probe outside of the targeting arm region and *Eco*RV digestion (Fig. 1). Chimeras from one clone (ES20) were crossed with WT C57Bl/6 mice, and F_1 offspring were genotyped by Southern blotting. Subsequent genotyping was performed by PCR detection of WT and KO alleles from tail

DNA extracts. Genotyping PCR primers for the WT allele were 5′-CTTTTCTCGGTAATTTAGCCTCAC-3′ and 5′-ATGT CGGGGATCTGTTTATTCA-3′, and those for the KO allele were 5′-CGGACCGCTATCAGGACA-3′ and 5′-AA GTGGGAATCAAGAGAAAAACA-3′. Mice were also genotyped for the CP49 gene as described previously [30].

Verification of KO

The expression of *Crygs* was assayed by RT-PCR with primers spanning exons 1–3 (forward, 5′-TCTCTCAGTA GTGCGGGAATCAACCT-3′; reverse, 5′-GGACCACAA GCCAGACAGCAGAG-3′). β-Actin expression was detected with the following primers: forward, 5′-CTG GCTGGCCGGGACCTGAC-3′; reverse, 5′-ACCGCTCG TTGCCAATAGTGATGA-3′.

Western blots

Lenses were homogenized in 50 μL per lens of NaCl/Tris, NaCl/Tris plus 1% Triton X-100, or NaCl/Tris plus 0.1% SDS. Supernatants after microcentrifugation were analyzed on 10% SDS/PAGE gels, and transferred to poly(vinylidene difluoride) membranes. For some experiments, the whole lens was homogenized in RIPA buffer, 50 mM Tris/HCl (pH 7.4), 150 mM NaCl, 0.25% deoxycholic acid, 1% NP-40, and 1 mM EDTA.

Two-dimensional electrophoresis was performed at Bioworld (Dublin, OH, USA) by the carrier ampholine method of IEF ([62], using reagents from Kendrick Labs (Madison, WI, USA), and blotting onto nitrocellulose.

For both PAGE and 2D electrophoresis, membranes were incubated with rabbit polyclonal antibody against mouse γS [20] at 1 : 10 000 and visualized by electrochemiluminescence (GE Healthcare, Piscataway, NJ, USA).

Imaging the mouse lens and optics

Lenses were freshly dissected in NaCl/P_i and positioned posterior side up in the beveled center hole (1.7 mm in diameter) of a black 1-mm thick plastic washer submerged in NaCl/P_i buffer in a 60-mm Petri dish on the stage of a Zeiss Stemi-2000C microscope (Göttingen, Germany). The stage and the Petri dish were sandwiched by a highly detailed image printed on a transparency film (stage side) and by a 10-mm spacer (a Petri dish cover). The images through the lens were recorded with a Canon A640 digital camera system with × 30 magnification and illumination from below.

SEM and TEM

For SEM, lenses were fixed in a mixture of 2% paraformaldehyde and 2.5% glutaraldehyde in 0.1 M sodium cacodylate buffer (EM fix) for 1 h. Lenses were split along the optic axis and fixed for a further 12 h. The tissue was dehydrated through acetone, critical point dried, and then split into quarters, yielding fresh fracture surfaces. Specimens were sputter-coated and examined with a scanning electron microscope (XL 30; Philips, Andover, MA, USA). For TEM, tissues were fixed and processed routinely as previously described [63].

Actin staining and quantitation

Frozen sections of eyes from littermate WT and KO mice were prepared as described previously [16] and stained with Alexa Fluor-488-conjugated phalloidin (1 : 100 in NaCl/P_i) with 1% BSA for 30 min at room temperature, counterstained with DAPI, and mounted with Prolong Gold antifade mounting medium (Invitrogen, Carlsbad, CA, USA). For quantitation, sections were also stained with 50 $\mu g \cdot mL^{-1}$ Alexa Fluor-488-conjugated DNaseI (Molecular

Probes, Carlsbad, CA, USA). Sections were washed, mounted and imaged at 488 nm (DNaseI), 568 nm (phalloidin) and 364 nm (DAPI) excitation wavelengths, with a Leica confocal microscope (TCS SP2) with a × 40 0.85 numerical aperture (HCX Plan Apo CS) and a × 40 0.75–1.25 numerical aperture (Oil HCX Plan Apo CS) objective lens (Leica, Deerfield, IL, USA). Images were analyzed with LEICA-LITE software (Leica), and signal intensities for 488 and 568 nm across the equatorial cortical region of the lens were plotted as a function of distance. The F-actin/G-actin ratios from different animals were averaged.

The F-actin/G-actin ratio was determined with an *in vivo* actin assay kit (Cytoskeleton, Denver, CO, USA). Separated G-actin and F-actin fractions were quantified after western blotting with 1 : 1000 anti-actin serum (Cytoskeleton), using IMAGEQUANT 5.2. The tubulin/microtubule ratio in native mouse lenses was similarly determined with the Microtubules/Tubulin *In Vivo* Assay Kit (Cytoskeleton), following the manufacturer's protocols.

For examination of copelleting of γS and F-actin, the whole WT lens was homogenized in LAS2 buffer (Cytoskeleton) and divided equally. One sample was treated with cytochalasin D (EMD4; Biosciences, Rockland, MA, USA) at a final concentration of 200 μM. Both samples were centrifuged at 100 000 ***g*** for 1 h, and supernatant and pellet fractions were examined by western blot with rabbit anti-γS serum.

F-actin/γS colocalization

Unfixed eyes from adult WT mice were embedded in Optical Cutting Temperature freezing medium and snap frozen in liquid nitrogen. Thick (150 μm) frozen sections were cut at −18 °C with a Leica Cryostat (CM3050), and 'ghosted' [64] to reduce soluble cytoplasmic proteins. Sections were fixed with 4% paraformaldehyde in $NaCl/P_i$ for 2 h, and stained sequentially (1 h at 4 °C) with rabbit polyclonal anti-γS serum, Alexa Fluor-568-conjugated phalloidin, and Alexa Fluor-488-conjugated anti-rabbit IgG and DAPI. After extensive washing, the stained sections were mounted and imaged under a confocal fluorescence microscope.

Mitochondrial and endoplasmic reticulum markers and intermediate filaments

Frozen sections of mouse lenses were labeled with mouse antibodies against COX IV (a mitochondrial marker) or PDI (an endoplasmic reticulum marker) (Abcam, Cambridge, MA, USA) at 1 : 200 dilution, or with rabbit polyclonal antibody against purified recombinant human CP49/phakinin/BFSP2 (1 : 1000 dilution), or rabbit polyclonal antibody against purified recombinant human CP94/filensin/BFSP1 (1 : 1000 dilution) [36], and visualized as described above.

Actin polymerization/depolymerization

For assays, we used the Actin Polymerization Biochem Kit BK003 (Cytoskeleton), based on the polymerization-dependent increase in fluorescence of pyrene-conjugated actin [37,38]. Ranges of concentrations of recombinant mouse γS [26] or BSA were added. Each experiment was performed in triplicate or quadruplicate. Relative fluorescence was plotted as a function of time.

Acknowledgments

This work was supported by the Intramural Program of the National Eye Institute and by NEI Core Grant P30 EY12576, UC Davis, and EY08747 to P. FitzGerald.

Abbreviations

DAPI	4′,6-diamidino-2-phenylindole
KO	knockout
SEM	scanning electron microscopy
TEM	transmission electron microscopy
WT	wild-type
γA	γA-crystallin
γB	γB-crystallin
γC	γC-crystallin
γD	γD-crystallin
γE	γE-crystallin
γF	γF-crystallin
γN	γN-crystallin
γS	γS-crystallin

References

1. Maisel, H.; Harding, CV.; Alcala, JR.; Kuszak, J.; Bradley, R.; Bloemendal, H. The morphology of the lens. In: Bloemendal, H., editor. Molecular and Cellular Biology of the Eye Lens. Wiley Interscience; New York: 1981. p. 49-84.
2. Harding, JJ.; Crabbe, MJC. The lens: development, proteins, metabolism and cataract. In: Davson, H., editor. The Eye. Academic Press; New York: 1984. p. 207-492.
3. Bron AJ, Vrensen GF, Koretz J, Maraini G, Harding JJ. The ageing lens. Ophthalmologica. 2000; 214:86–104. [PubMed: 10657747]
4. Bassnett S. On the mechanism of organelle degradation in the vertebrate lens. Exp Eye Res. 2009; 88:133–139. [PubMed: 18840431]
5. Kuszak JR, Zoltoski RK, Sivertson C. Fibre cell organization in crystalline lenses. Exp Eye Res. 2004; 78:673–687. [PubMed: 15106947]
6. Wyatt K, Gao C, Tsai JY, Fariss RN, Ray S, Wistow G. A role for lengsin, a recruited enzyme, in terminal differentiation in the vertebrate lens. J Biol Chem. 2008; 283:6607–6615. [PubMed: 18178558]
7. Grey AC, Jacobs MD, Gonen T, Kistler J, Donaldson PJ. Insertion of MP20 into lens fibre cell plasma membranes correlates with the formation of an extracellular diffusion barrier. Exp Eye Res. 2003; 77:567–574. [PubMed: 14550398]
8. Wistow, G. Molecular Biology and Evolution of Crystallins: Gene Recruitment and Multifunctional Proteins in the Eye Lens. R.G. Landes Company; Austin, TX: 1995.
9. Wistow GJ, Mulders JW, de Jong WW. The enzyme lactate dehydrogenase as a structural protein in avian and crocodilian lenses. Nature. 1987; 326:622–624. [PubMed: 3561501]
10. de Jong WW, Hendriks W, Mulders JW, Bloemendal H. Evolution of eye lens crystallins: the stress connection. Trends Biochem Sci. 1989; 14:365–368. [PubMed: 2688200]
11. Wistow G. Lens crystallins: gene recruitment and evolutionary dynamism. Trends Biochem Sci. 1993; 18:301–306. [PubMed: 8236445]
12. Wistow GJ, Piatigorsky J. Lens crystallins: the evolution and expression of proteins for a highly specialized tissue. Annu Rev Biochem. 1988; 57:479–504. [PubMed: 3052280]
13. Ingolia TD, Craig EA. Four small Drosophila heat shock proteins are related to each other and to mammalian α-crystallin. Proc Natl Acad Sci USA. 1982; 79:2360–2364. [PubMed: 6285380]

14. de Jong WW, Caspers GJ, Leunissen JA. Genealogy of the alpha-crystallin–small heat-shock protein superfamily. Int J Biol Macromol. 1998; 22:151–162. [PubMed: 9650070]
15. Horwitz J. α-Crystallin can function as a molecular chaperone. Proc Natl Acad Sci USA. 1992; 89:10449–10453. [PubMed: 1438232]
16. Wistow G, Wyatt K, David L, Gao C, Bateman O, Bernstein S, Tomarev S, Segovia L, Slingsby C, Vihtelic T. gammaN-crystallin and the evolution of the betagamma-crystallin superfamily in vertebrates. FEBS J. 2005; 272:2276–2291. [PubMed: 15853812]
17. Shimeld SM, Purkiss AG, Dirks RP, Bateman OA, Slingsby C, Lubsen NH. Urochordate betagamma-crystallin and the evolutionary origin of the vertebrate eye lens. Curr Biol. 2005; 15:1684–1689. [PubMed: 16169492]
18. Wistow G. Evolution of a protein superfamily: relationships between vertebrate lens crystallins and microorganism dormancy proteins. J Mol Evol. 1990; 30:140–145. [PubMed: 2107329]
19. Ray ME, Wistow G, Su YA, Meltzer PS, Trent JM. AIM1, a novel non-lens member of the betagamma-crystallin superfamily, is associated with the control of tumorigenicity in human malignant melanoma. Proc Natl Acad Sci USA. 1997; 94:3229–3234. [PubMed: 9096375]
20. Sinha D, Esumi N, Jaworski C, Kozak CA, Pierce E, Wistow G. Cloning and mapping the mouse Crygs gene and non-lens expression of [gamma]S-crystallin. Mol Vis. 1998; 4:8–15. [PubMed: 9565648]
21. Organisciak D, Darrow R, Barsalou L, Rapp C, McDonald B, Wong P. Light induced and circadian effects on retinal photoreceptor cell crystallins. Photochem Photobiol. 2011; 87:151–159. [PubMed: 21091955]
22. Tian J, Ishibashi K, Reiser K, Grebe R, Biswal S, Gehlbach P, Handa JT. Advanced glycation endproduct-induced aging of the retinal pigment epithelium and choroid: a comprehensive transcriptional response. Proc Natl Acad Sci USA. 2005; 102:11846–11851. [PubMed: 16081535]
23. Crabb JW, Miyagi M, Gu X, Shadrach K, West KA, Sakaguchi H, Kamei M, Hasan A, Yan L, Rayborn ME, et al. Drusen proteome analysis: an approach to the etiology of age-related macular degeneration. Proc Natl Acad Sci USA. 2002; 99:14682–14687. [PubMed: 12391305]
24. Umeda S, Suzuki MT, Okamoto H, Ono F, Mizota A, Terao K, Yoshikawa Y, Tanaka Y, Iwata T. Molecular composition of drusen and possible involvement of anti-retinal autoimmunity in two different forms of macular degeneration in cynomolgus monkey (Macaca fascicularis). FASEB J. 2005; 19:1683–1685. [PubMed: 16099945]
25. Bu L, Yan S, Jin M, Jin Y, Yu C, Xiao S, Xie Q, Hu L, Xie Y, Solitang Y, et al. The gamma S-crystallin gene is mutated in autosomal recessive cataract in mouse. Genomics. 2002; 80:38–44. [PubMed: 12079281]
26. Sinha D, Wyatt MK, Sarra R, Jaworski C, Slingsby C, Thaung C, Pannell L, Robison WG, Favor J, Lyon M, et al. A temperature-sensitive mutation of Crygs in the murine Opj cataract. J Biol Chem. 2001; 276:9308–9315. [PubMed: 11121426]
27. Sun H, Ma Z, Li Y, Liu B, Li Z, Ding X, Gao Y, Ma W, Tang X, Li X, et al. Gamma-S crystallin gene (CRYGS) mutation causes dominant progressive cortical cataract in humans. J Med Genet. 2005; 42:706–710. [PubMed: 16141006]
28. Lee S, Mahler B, Toward J, Jones B, Wyatt K, Dong L, Wistow G, Wu Z. A single destabilizing mutation (F9S) promotes concerted unfolding of an entire globular domain in gammaS-crystallin. J Mol Biol. 2010; 399:320–330. [PubMed: 20382156]
29. Mahler B, Doddapaneni K, Kleckner I, Yuan C, Wistow G, Wu Z. Characterization of a transient unfolding intermediate in a core mutant of gammaS-crystallin. J Mol Biol. 2011; 405:840–850. [PubMed: 21108948]
30. Sandilands A, Wang X, Hutcheson AM, James J, Prescott AR, Wegener A, Pekny M, Gong X, Quinlan RA. Bfsp2 mutation found in mouse 129 strains causes the loss of CP49′ and induces vimentin-dependent changes in the lens fibre cell cytoskeleton. Exp Eye Res. 2004; 78:875–889. [PubMed: 15037121]
31. Alizadeh A, Clark J, Seeberger T, Hess J, Blankenship T, FitzGerald PG. Characterization of a mutation in the lens-specific CP49 in the 129 strain of mouse. Invest Ophthalmol Vis Sci. 2004; 45:884–891. [PubMed: 14985306]

32. Wistow GJ, Shaughnessy MP, Lee DC, Hodin J, Zelenka PS. A macrophage migration inhibitory factor is expressed in the differentiating cells of the eye lens. Proc Natl Acad Sci USA. 1993; 90:1272–1275. [PubMed: 7679497]
33. Ueda Y, Duncan MK, David LL. Lens proteomics: the accumulation of crystallin modifications in the mouse lens with age. Invest Ophthalmol Vis Sci. 2002; 43:205–215. [PubMed: 11773033]
34. Takemoto L. Deamidation of Asn-143 of gamma S crystallin from protein aggregates of the human lens. Curr Eye Res. 2001; 22:148–153. [PubMed: 11402392]
35. FitzGerald PG. Lens intermediate filaments. Exp Eye Res. 2009; 88:165–172. [PubMed: 19071112]
36. Sandilands A, Prescott AR, Hutcheson AM, Quinlan RA, Casselman JT, FitzGerald PG. Filensin is proteolytically processed during lens fiber cell differentiation by multiple independent pathways. Eur J Cell Biol. 1995; 67:238–253. [PubMed: 7588880]
37. Kumar N, Tomar A, Parrill AL, Khurana S. Functional dissection and molecular characterization of calcium-sensitive actin-capping and actin-depolymerizing sites in villin. J Biol Chem. 2004; 279:45036– 45046. [PubMed: 15272027]
38. Takamiya R, Takahashi M, Park YS, Tawara Y, Fujiwara N, Miyamoto Y, Gu J, Suzuki K, Taniguchi N. Overexpression of mutated Cu,Zn-SOD in neuroblastoma cells results in cytoskeletal change. Am J Physiol Cell Physiol. 2005; 288:C253–C259. [PubMed: 15456693]
39. Kappe G, Purkiss AG, van Genesen ST, Slingsby C, Lubsen NH. Explosive expansion of betagamma-crystallin genes in the ancestral vertebrate. J Mol Evol. 2010; 71:219–230. [PubMed: 20725717]
40. Bloemendal H, De Jong W, Jaenicke R, Lubsen NH, Slingsby C, Tardieu A. Ageing and vision: structure, stability and function of lens crystallins. Prog Biophys Mol Biol. 2004; 86:407–485. [PubMed: 15302206]
41. Brakenhoff RH, Aarts HJ, Reek FH, Lubsen NH, Schoenmakers JG. Human gamma-crystallin genes. A gene family on its way to extinction. J Mol Biol. 1990; 216:519–532. [PubMed: 2258929]
42. Wistow G, Bernstein SL, Wyatt MK, Behal A, Touchman JW, Bouffard G, Smith D, Peterson K. Expressed sequence tag analysis of adult human lens for the NEIBank Project: over 2000 non-redundant transcripts, novel genes and splice variants. Mol Vis. 2002; 8:171–184. [PubMed: 12107413]
43. Simpanya MF, Wistow G, Gao J, David LL, Giblin FJ, Mitton KP. Expressed sequence tag analysis of guinea pig (Cavia porcellus) eye tissues for NEIBank. Mol Vis. 2008; 14:2413–2427. [PubMed: 19104676]
44. Wang X, Garcia CM, Shui YB, Beebe DC. Expression and regulation of alpha-, beta-, and gamma-crystallins in mammalian lens epithelial cells. Invest Ophthalmol Vis Sci. 2004; 45:3608–3619. [PubMed: 15452068]
45. Jaworski C, Wistow G. LP2, a differentiation-associated lipid-binding protein expressed in bovine lens. Biochem J. 1996; 320(Pt 1):49–54. [PubMed: 8947466]
46. Wu Z, Delaglio F, Wyatt K, Wistow G, Bax A. Solution structure of (gamma)S-crystallin by molecular fragment replacement NMR. Protein Sci. 2005; 14:3101– 3114. [PubMed: 16260758]
47. Zhang J, Li J, Huang C, Xue L, Peng Y, Fu Q, Gao L, Li W. Targeted knockout of the mouse betaB 2-crystallin gene (Crybb2) induces age-related cataract. Invest Ophthalmol Vis Sci. 2008; 49:5476–5483. [PubMed: 18719080]
48. Ishizaki Y, Jacobson MD, Raff MC. A role for caspases in lens fiber differentiation. J Cell Biol. 1998; 140:153–158. [PubMed: 9425163]
49. Bassnett S, Mataic D. Chromatin degradation in differentiating fiber cells of the eye lens. J Cell Biol. 1997; 137:37–49. [PubMed: 9105035]
50. Nishimoto S, Kawane K, Watanabe-Fukunaga R, Fukuyama H, Ohsawa Y, Uchiyama Y, Hashida N, Ohguro N, Tano Y, Morimoto T, et al. Nuclear cataract caused by a lack of DNA degradation in the mouse eye lens. Nature. 2003; 424:1071–1074. [PubMed: 12944971]
51. Sandilands A, Prescott AR, Carter JM, Hutcheson AM, Quinlan RA, Richards J, FitzGerald PG. Vimentin and CP49/filensin form distinct networks in the lens which are independently modulated during lens fibre cell differentiation. J Cell Sci. 1995; 108(Pt 4):1397–1406. [PubMed: 7615661]

52. Cavey M, Lecuit T. Molecular bases of cell–cell junction stability and dynamics. Cold Spring Harb Perspect Biol. 2009; 1:a002998. [PubMed: 20066121]
53. Bassnett S, Wilmarth PA, David LL. The membrane proteome of the mouse lens fiber cell. Mol Vis. 2009; 15:2448–2463. [PubMed: 19956408]
54. Liu SB, He YY, Zhang Y, Lee WH, Qian JQ, Lai R, Jin Y. A novel non-lens betagamma-crystallin and trefoil factor complex from amphibian skin and its functional implications. PLoS One. 2008; 3:e1770. [PubMed: 18335045]
55. Takabatake T, Takahashi TC, Takeshima K. Cloning of an epidermis-specific Cynops cDNA from a neurula library. Dev Growth Differ. 1992; 34:277–283.
56. Wistow G, Jaworski C, Rao PV. A non-lens member of the beta gamma-crystallin superfamily in a vertebrate, the amphibian Cynops. Exp Eye Res. 1995; 61:637–639. [PubMed: 8654507]
57. Bloemendal, H.; Berbers, GAM.; De Jong, WW.; Ramaekers, F.; Vermorken, AJM.; Dunia, I.; Benedetti, EL. Interaction of crystallins with the cytoskeletal–plasma membrane complex of the bovine lens. In: Nugent, J.; Whelan, J., editors. Human Cataract Formation; Ciba Foundation Symposium; London, UK: Pitman Press; 1984. p. 177-190.
58. Verschuure P, Croes Y, van den Ijessel PR, Quinlan RA, de Jong WW, Boelens WC. Translocation of small heat shock proteins to the actin cytoskeleton upon proteasomal inhibition. J Mol Cell Cardiol. 2002; 34:117–128. [PubMed: 11851352]
59. Andley UP. Effects of alpha-crystallin on lens cell function and cataract pathology. Curr Mol Med. 2009; 9:887–892. [PubMed: 19860667]
60. Delaye M, Tardieu A. Short-range order of crystallin proteins accounts for eye lens transparency. Nature. 1983; 302:415–417. [PubMed: 6835373]
61. Mansour SL, Thomas KR, Capecchi MR. Disruption of the proto-oncogene int-2 in mouse embryo-derived stem cells: a general strategy for targeting mutations to non-selectable genes. Nature. 1988; 336:348–352. [PubMed: 3194019]
62. O'Farrell PH. High resolution two-dimensional electrophoresis of proteins. J Biol Chem. 1975; 250:4007–4021. [PubMed: 236308]
63. Alizadeh A, Clark J, Seeberger T, Hess J, Blankenship T, FitzGerald PG. Targeted deletion of the lens fiber cell-specific intermediate filament protein filensin. Invest Ophthalmol Vis Sci. 2003; 44:5252–5258. [PubMed: 14638724]
64. Yoon KH, Blankenship T, Shibata B, Fitzgerald PG. Resisting the effects of aging: a function for the fiber cell beaded filament. Invest Ophthalmol Vis Sci. 2008; 49:1030–1036. [PubMed: 18326727]

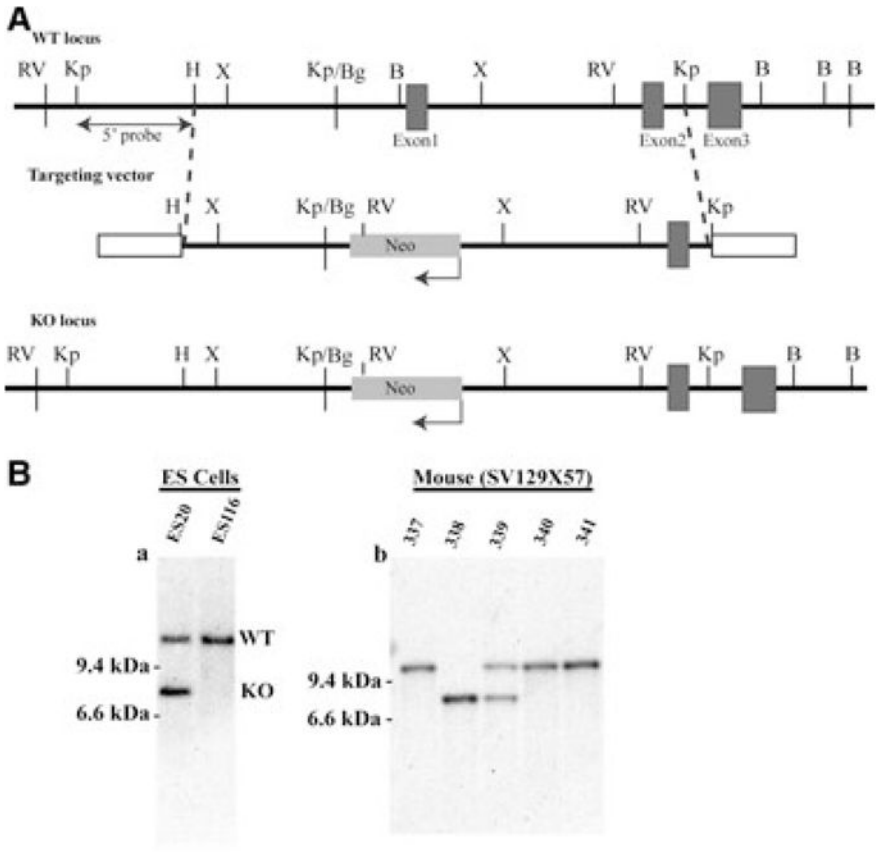

Fig. 1.

Construction of the *Crygs* null allele. (A) Summary diagram of the deletion strategy. The genomic organization of the mouse *Crygs* locus is shown at the top. The targeting vector used to generate the null allele is shown in the middle, in which a *Neo* resistance gene (*Neo*^{R}) driven by the phosphoglycerate kinase promoter is used to replace the 5′-flanking region and exon 1 of the *Crygs* gene. The bottom panel shows integration of the targeting vector at the target locus through homologous recombination. Restriction sites are indicated as follows: RV, *Eco*RV; Kp, *Kpn*I; H, *Hin*dIII; X, *Xho*I;, Bg, *Bgl*II; B, *Bam*HI. (B) Southern blot analysis of the *Crygs* targeted allele. Genomic DNA from ES clones and F_1 germline mouse tails was digested with *Eco*RV and probed with a probe upstream of the 5′-target region, as shown in (A). Bands corresponding to WT and KO loci are indicated.

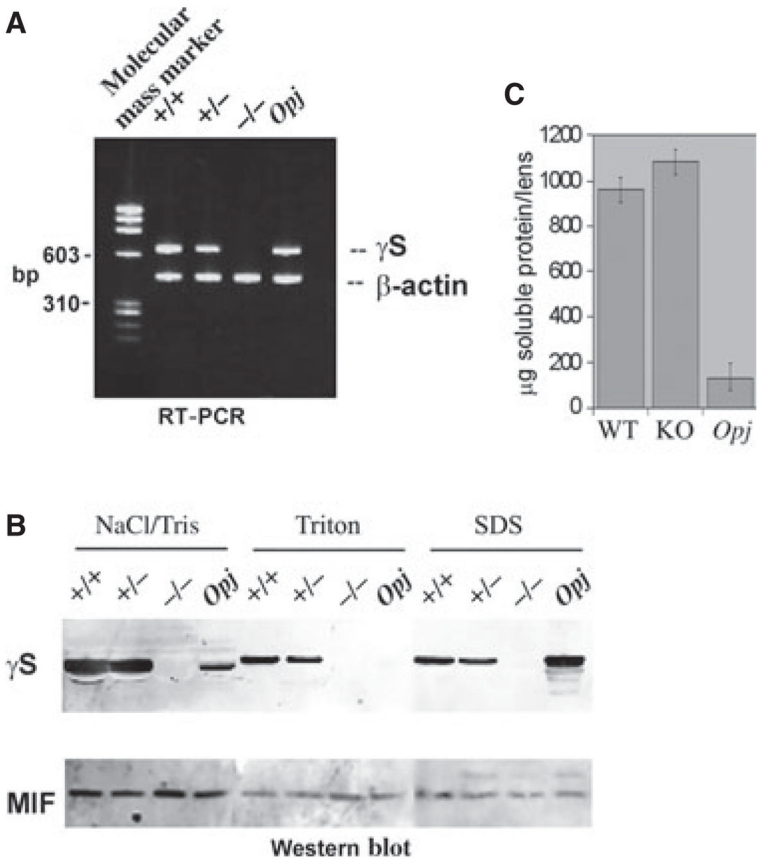

Fig. 2.

Validation of loss of γS expression. (A) RT-PCR of lenses from WT (+/+), heterozygous (+/−), KO (−/−) and *Opj* mice show absence of mRNA for γS in the KO mouse. β-Actin was used as positive control. (B) Western blot of lenses from WT (+/+), heterozygous (+/−), KO (−/−) and *Opj* mice. Lens extracts were fractionated into NaCl/Tris-soluble, Triton-soluble and SDS-soluble fractions. Blots were hybridized with antibodies against γS and MIF (as loading control). (C) Total soluble protein per lens was measured for three pairs each of age-matched WT, KO and *Opj* mice. There was no significant difference in content between WT and KO lenses.

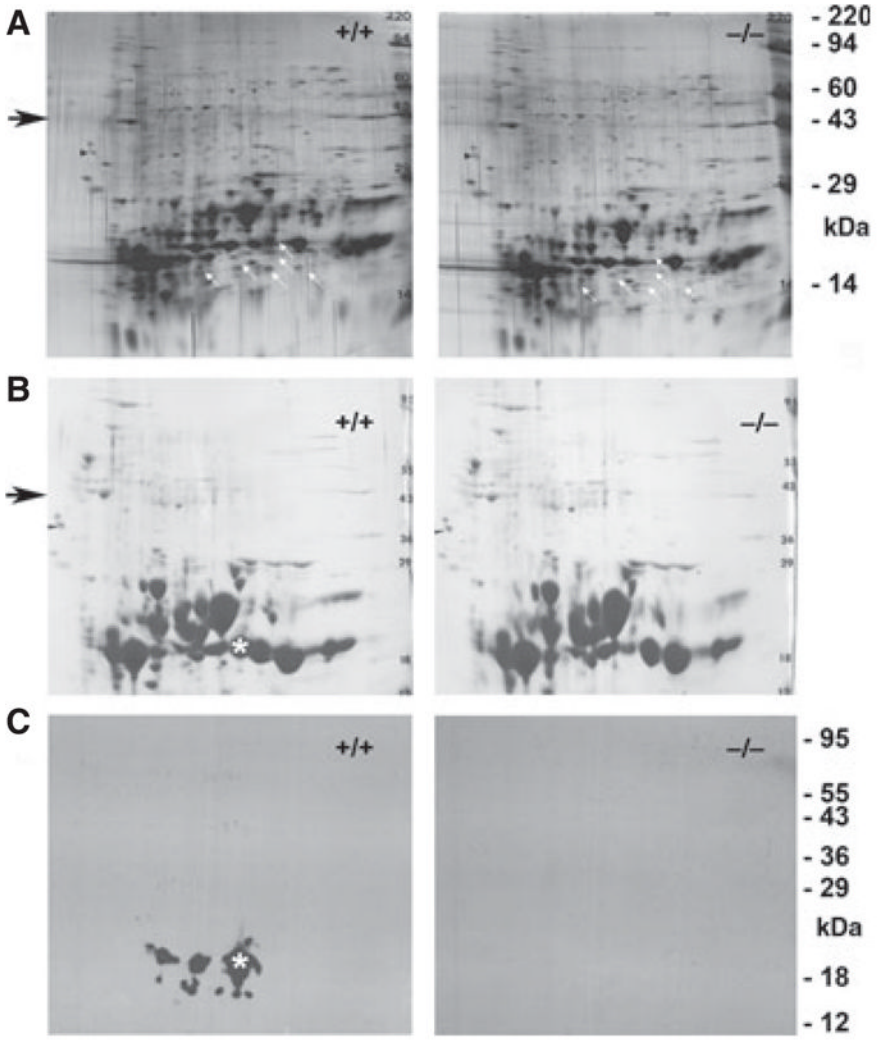

Fig. 3.

Two-dimensional gel electrophoresis of WT and KO mouse lenses. (A) Silver-stained blots of WT and KO lenses. White arrows indicate the positions of spots missing in the KO lens. The black arrow indicates the size region for actin. (B) Coomassie stain and (C) western blot of γS for duplicate 2D gels of WT and KO lenses. The asterisk shows the position of the main γS spot. The WT lens shows evidence of multiple post-translational modifications of γS, whereas the KO lens shows complete absence of γS immunoreactivity.

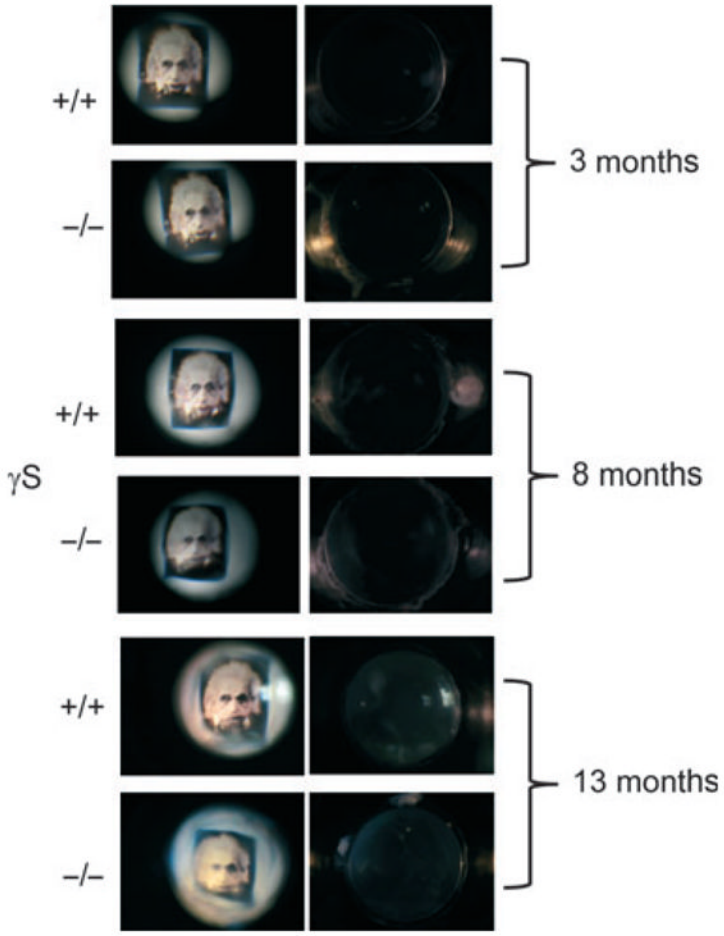

Fig. 4.

Defective optics in the aging γS KO lens. Representative images for aged-matched WT and KO lenses. The panels on the right show dark field photographs of WT and KO lenses. KO lenses are transparent even up to 13 months, with no more than slight haziness. The panels on the left show images taken through the lenses under identical conditions. At 3 months, there are no differences between WT and KO lenses, but by 8 months, image formation in the KO lens is noticeably worse.

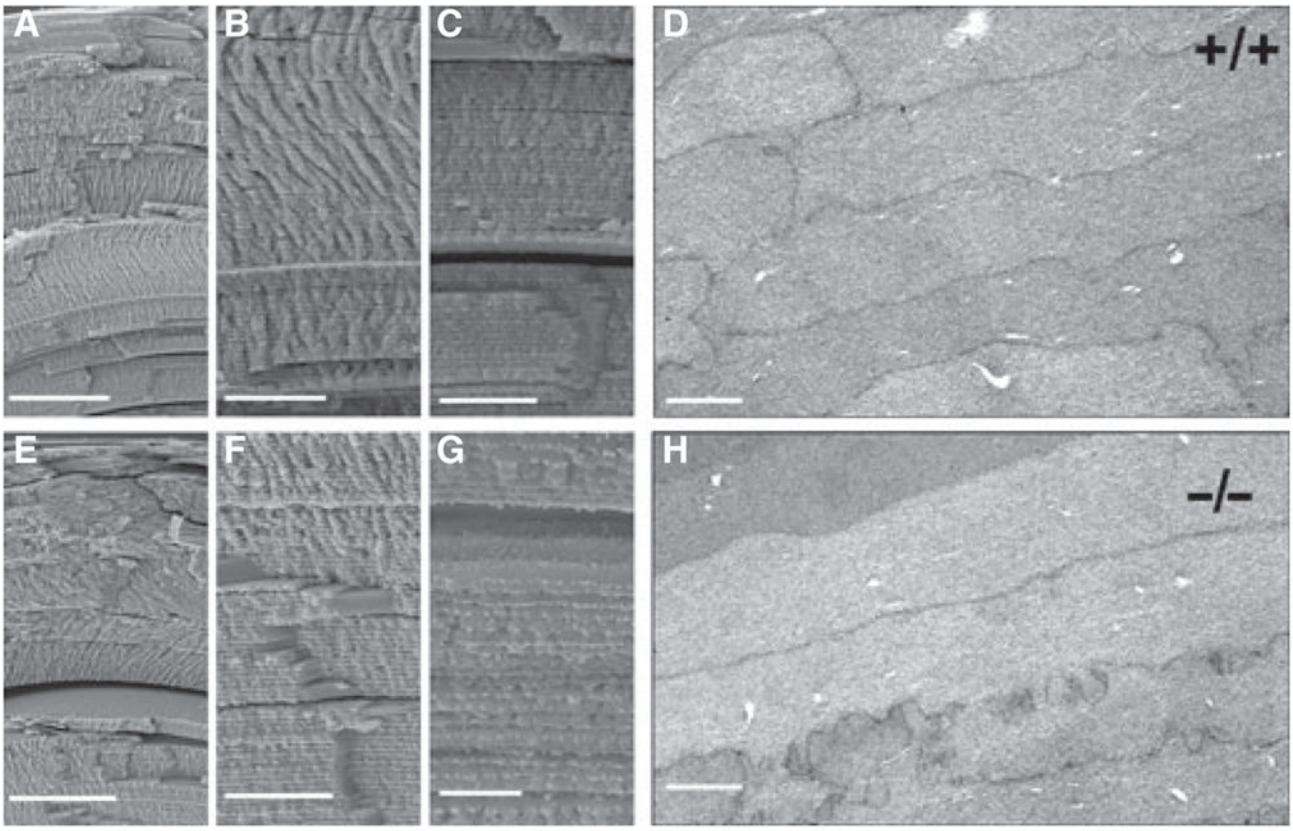

Fig. 5.

Organization of fiber cells in the γS KO lens appears normal by electron microscopy. In each row, the first three panels (A–C; E–G) show SEM images of the lens cortex. (D) and (H) show TEM images of cortical fiber cells. Images are from 6-month-old littermate lenses, with the WT lens above and the KO lens below. Size bars: (A) 100 μm; (B) 25 μm; (C) 25 μm; (D) 2 μm; (E) 100 μm; (F) 25 μm; (G) 10 μm; (H) 2 μm. No significant differences were observed.

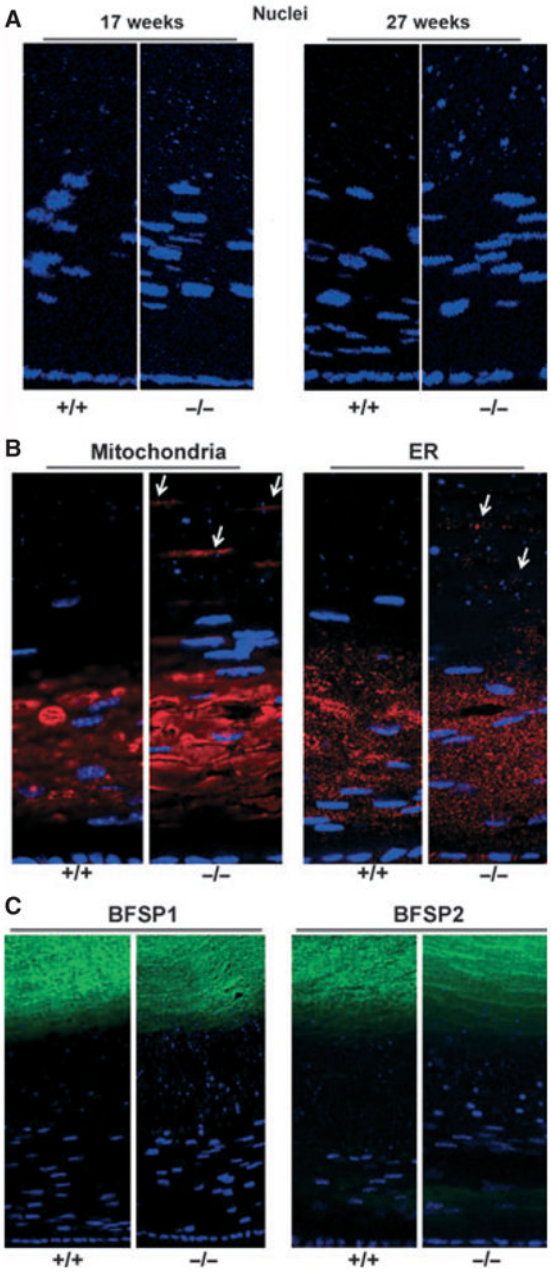

Fig. 6.

Inefficient clearance of organelles in the γS KO lens. (A) Nuclei. DAPI staining of sections from 17-week-old and 27-week-old littermate lenses for WT (+/+) and KO (−/−) mice. KO lenses showed increased levels of DAPI-stained nuclei and condensed nuclear fragments in mature fiber cells. Similar results are also apparent in (B) and in Fig. 8. (B) Other organelles. Immunofluorescent labeling of 6-month-old WT (+/+) and KO (−/−) lenses for a mitochondrial marker (COX IV) (left panels) and an endoplasmic reticulum (ER) marker (PDI) (right panels). In the KO lens, immunoreactivity for the organelle markers persisted in mature fiber cell layers. (C) Intermediate filaments. Immunofluorescent labeling for the lens-specific intermediate filaments BFSP1 (filensin) and BFSP2 (CP49) in 8-month-old lenses. No obvious differences were seen between WT (+/+) and KO (−/−) lenses.

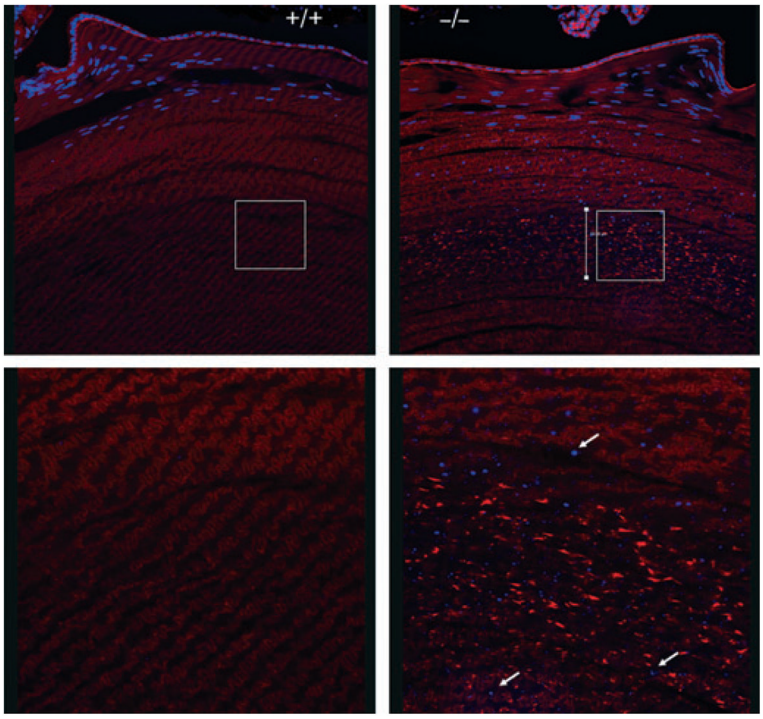

Fig. 7.

Histology of γS KO and WT lenses reveals defects in nuclear breakdown and the organization of F-actin. DAPI (blue) stain for nuclei/chromatin and phalloidin (red) stain for F-actin. The upper panels show sections of lens from the epithelium into the deep cortex. The lower panels show magnified views of the equivalent deep cortical regions indicated by white squares in the upper panel. Size bar: 100 μm. Arrows highlight chromatin bodies in the deep cortex. The KO lens shows retention of nuclear fragments deep into the lens, and a discrete zone with clumping of F-actin.

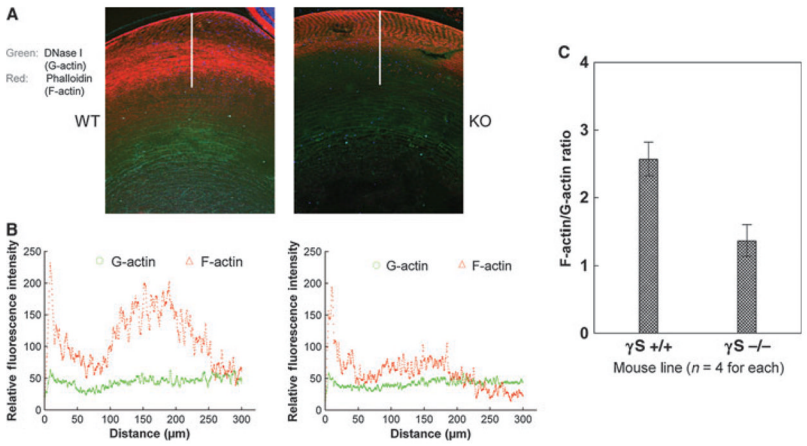

Fig. 8.

Changes in F-actin/G-actin ratio in the γS KO lens. Comparative scanning of labeling for F-actin (red) and G-actin (green) in WT and KO lenses. (A) Typical staining patterns for WT and KO lenses. The line shows the 300-μm scan line. (B) Typical examples of the intensity scans for red and green channels through the lens cortex. (C) The averaged F-actin/G-actin ratios through the cortex for WT (+/+) and KO (−/−) lenses ($n = 4$). Overall, the F-actin/G-actin intensity ratio for the KO lens is approximately half of that for the WT lens.

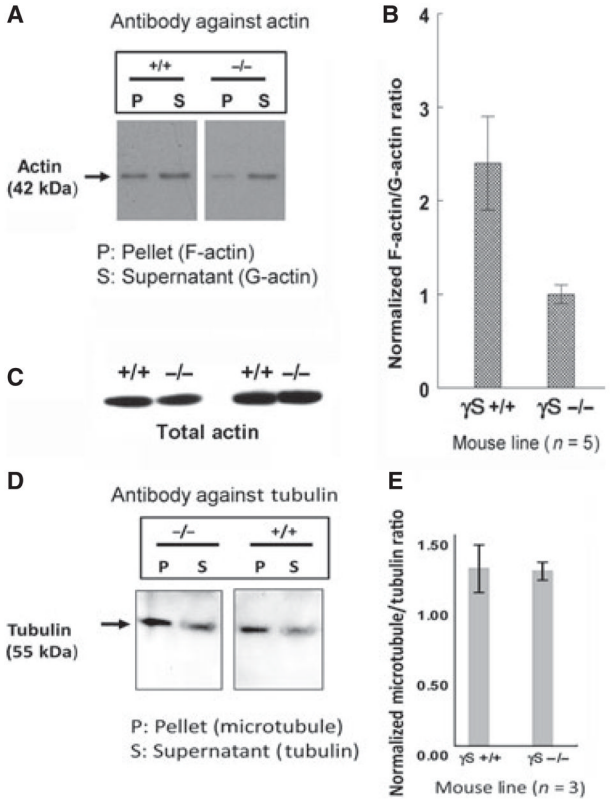

Fig. 9.

Changes in F-actin/G-actin ratio in the γS KO lens. P (pellet) and S (supernatant) actin fractions were separated from WT (+/+) and KO (−/−) lenses. (A) Western blots for actin for a typical example. (B) Summary of results for five pairs of WT and KO mice, showing error bars. Overall, the F-actin/G-actin ratio for the KO lens is about half that for the WT lens. (C) Western blots for total actin from two littermate pairs of +/+ and −/− mice, extracted in RIPA buffer. There is no significant difference in overall actin levels. Filamentous (pellet, P) and monomeric (supernatant, S) tubulins were separated from matched WT and KO lenses ($n = 3$). (D) Western blots for tubulin for typical examples. (E) Summary of results for WT and KO mice. There was no significant difference between WT and KO lenses.

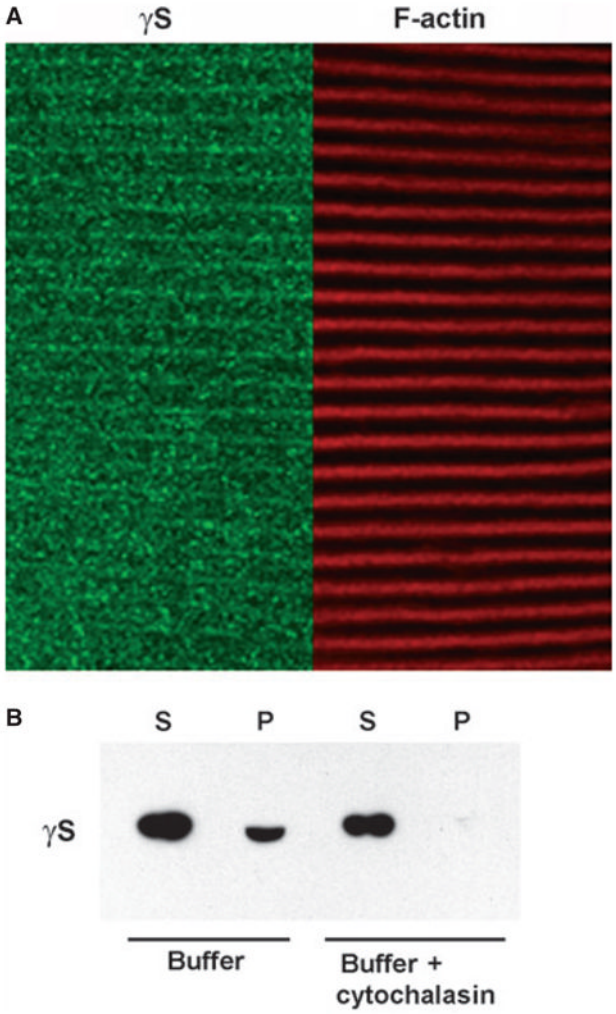

Fig. 10.

Association of γS and F-actin in lenses. (A) Colocalization of γS and F-actin in lens cortical fibers. Thick sections of a 6-month-old WT lens were 'ghosted' and labeled with phalloidin (red) for F-actin and with antibody against γS (green). The panels show aligned images for F-actin and γS. Signals colocalize along the plasma membrane of the elongated fiber cells. (B) Western blot of γS in the supernatant (S) and pellet (P) of whole lens extract centrifuged at 100 000 ***g*** for 1 h with and without addition of cytochalasin D. The supernatant, containing most of the γS, was loaded at 1/20 of the volume of the pellet. The presence of γS in the pellet was abolished by addition of cytochalasin D.

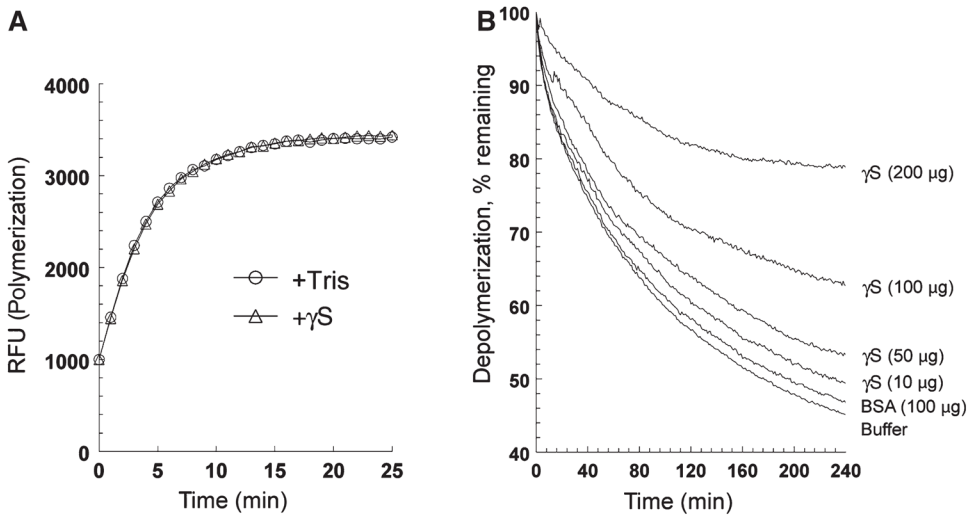

Fig. 11.

Recombinant mouse γS stabilizes F-actin *in vitro*. (A) Effect of added recombinant mouse γS (100 μg) on polymerization of pyrene–actin as compared with buffer alone. Polymerization was determined according to increasing pyrene fluorescence. No effect of added protein was seen. (B) Effect of increasing amounts of added recombinant mouse γS (10–200 μg) on depolymerization of pyrene–actin as compared with buffer alone and with 100 μg of BSA. Polymerization was determined according to increasing pyrene fluorescence. Added γS protected F-actin in a concentration-dependent manner.